journal

J. Am. Ceram. Soc., 95 [8] 2614–2621 (2012)
DOI: 10.1111/j.1551-2916.2012.05292.x

Thermal Cycling of Suspension Plasma Sprayed Alumina-YSZ Coatings Containing Amorphous Phases

Fariba Tarasi,[‡,†] Mamoun Medraj,[‡] Ali Dolatabadi,[‡] Rogerio S. Lima,[§] and Christian Moreau[§]

[‡]Department of Mechanical and Industrial Engineering, Concordia University, Montreal, QC, Canada

[§]Industrial Materials Institute of National Research Council of Canada (IMI-NRC), Boucherville, QC, Canada

Thermal cyclic test at 1080°C for various numbers of cycles was performed on suspension plasma-sprayed coatings of alumina-yttria-stabilized zirconia composites and yttria-stabilized zirconia (YSZ). The structural variations of composite coatings were studied to verify the possibility of production of nano-composite coatings with nano-dispersed oxides. The results showed that this composite exhibited a lower thermally grown oxide growth than that of the YSZ. New multi-constituent composites formed of alternative regions of nano-precipitates of alumina in zirconia matrix and nano-precipitates of zirconia in alumina matrix were developed via phase transformation through thermal cyclic process of amorphous-containing structure.

I. Introduction

New generation of high efficiency gas turbine engines for aerospace, energy, and marine applications are designed to work at higher operating temperatures. However, direct exposure to high temperature service results in short life of the parts, such as, combustors, blades, and vanes. Following several decades of effort for enhancement of the metallic construction material, ceramic thermal barrier coatings (TBCs) have been a great step forward enabling the raise in service temperature.

A TBC system is usually composed of a top coat and a bond coat. The top coat is normally zirconia, stabilized with yttria (YSZ), ceria or some other oxides.[1,2] It reduces the high service temperature to what the substrate can withstand without failing by creep and/or thermal fatigue. The bond coat consisting of MCrAlY alloys reduces the thermal expansion mismatch between the substrate and the bond coat, protects the substrate against oxidation and finally forms a protective oxide known as thermally grown oxide layer (TGO). TGO is, in fact, the oxidation product of the bond coat and is composed of mostly α-alumina.[3] The TGO may co-exist with a porous layer of transient mixed oxides (spinels) of $(Cr, Al)_2O_3{\cdot}Ni(Cr, Al)_2O_4{\cdot}NiO$, which is detrimental to the durability of the coating system.[4] Cyclic heating of the coating normally results in extensive growth of the TGO, which can eventually cause the failure of the TBC through the mechanisms explained by fracture mechanics. TBC-coated parts, such as turbine blades are mainly used in severe thermal cyclic service conditions, which demand for verification of performance of every new coating developed to operate at these conditions.

Recently, alumina-zirconia composite ceramics have attracted extensive research[5–9] as a potential TBC choice of top coat material to substitute the presently used zirconia. Mainly deposited by plasma spray processes, these composites have shown the capability of larger temperature drop in the substrate from the coating surface and superior thermal shock resistance than YSZ.[10] Moreover, it has been demonstrated that composites of alumina with zirconia possess lower residual stresses,[11] higher hardness, and lower porosity levels, as well as, improved adhesion.[12]

On the other hand, during plasma spray deposition, besides formation of the thin alternating splats, the rapid solidification of molten ceramics, under specific conditions, form metastable and amorphous phases.[13,14] It is shown in the present study that a nano-composite can be created by post annealing of this amorphous phase of alumina-zirconia that may provide the favorable thermal and mechanical properties for several applications.

The suspension plasma spray (SPS) process as a method for production of nano-structured coatings was employed for deposition of nano- and micrometer-sized powders of alumina and YSZ in a liquid suspension as the carrier of the feed powder. To increase the chances of amorphous phase formation, the pseudo-eutectic composition of the alumina-YSZ system is chosen.

Accordingly, the goal of this research was first to investigate the performance of the new composite of SPS deposited alumina-YSZ under thermal cyclic testing and as compared with YSZ coated with the same process. The second aim of the study was to trace the structural changes during thermal cyclic testing and to present the know-how of fabrication of a mixed dispersed ceramic nano-composite as introduced by Kirsten *et al.*[15] which is composed of the two composites of alumina toughened zirconia (ATZ)[16] and zirconia toughened alumina (ZTA)[17] with their respective industrial applications.

II. Experimental Procedure

(1) Coating Deposition and Powder Characteristics

Suspension plasma spray process was employed to produce dense and porous coatings using an axial injection plasma torch (Axial III; Northwest Mettech, North Vancouver, BC, Canada) of suspension into plasma jet, as per the details mentioned elsewhere.[13,18] Two different powders were mixed to form pseudo-eutectic composition of alumina-8 wt% YSZ and were sprayed. In addition, one 8 wt% YSZ powder as the reference material was sprayed. Powder mixtures with a weight ratio of 60/40 for alumina-8 wt% YSZ were produced in two different size ranges including nano- and micrometer-size. Table I summarizes the details of the feed powders and the sprayed mixtures and presents an abbreviated name for them.

The resulting mixtures were suspended in ethanol with a solid concentration of 25–30 wt%. The suspensions were prepared as per the details mentioned elsewhere.[19] Coating samples were deposited on the Inconel 625 substrates over a

T. Troczynski—contributing editor

Manuscript No. 30762. Received January 12, 2012; approved April 28, 2012.
[†]Author to whom correspondence should be addressed. e-mail: f_tarasi@yahoo.com

Table I. Characteristics of the Powders used in Feed Suspensions

Powder size range	Feed powder mixture detail	Abbreviated Name
Micrometer-size mixed alumina-YSZ	Alumina 95% pure (Malakoff, TX, USA; average size 1.4 μm) + [(13 wt% YSZ (Unitec Norwal, CT, USA; average size 1.5 μm) + 5 wt% YSZ (Tosoh, Grove City, OH, USA; average size 2 μm)]	MAZ
Nano-size mixed alumina-YSZ	Alumina (Nanoamor Advanced Ceramic Materials Inc., Houston, TX. USA; 23–47 nm) + (13 wt% YSZ + 5 wt% YSZ) (both Inframat Advanced Materials, Farmington, CT, USA; 30–60 nm)	NAZ
Nano-size 8 wt% YSZ	(13 wt% YSZ + 5 wt% YSZ) (both Inframat Advanced Materials, Farmington, CT, USA; 30–60 nm)	NZ

bound coat of about 200 μm thickness of CoNiCrAlY, which was deposited using high velocity oxy-fuel process (HVOF).

The SPS spray condition used for deposition of each powder mixture are listed in Table II. The spray parameters were selected differently i.e., the micrometer-size powder is sprayed at higher plasma power to guarantee appropriate melting, due to higher temperature. The detail includes the plasma gas composition, the spray robot speed, and the plasma power. The suspensions were injected into plasma jet with a flow rate of 1.5 kg/h and sprayed at a distance of 50 mm from the substrate. A 4 mm step for each consecutive deposition row was used for complete coverage of the surface with the coating. A maximum substrate temperature of 400°C was maintained, during the spray process, using the interpass pauses, front air jet and back N_2 gas jet cooling.

Table II also shows the resulting in-flight particle temperatures and velocities, as well as, the consequent coating thicknesses per deposition passes. The particle temperatures and velocities were measured along the center line of the torch at spray distance using particle monitoring system (Accuraspray G3; Tecnar Automation, St. Bruno, QC, Canada). To achieve the same approximate coating thickness, monolithic 8 wt% YSZ required a larger number of deposition passes (90 passes) than the composite powder (60 passes), due to higher density of 8 wt% YSZ.

(2) Thermal Cycle Testing

Thermal cyclic tests of the resulting coatings were performed up to 500 cycles. The cycles included heating the samples in a heating element furnace under air atmosphere to 1080°C in a 15-min time period, holding at the test temperature for 1 h to allow homogenous temperature profile through the coatings, and then air jet cooling down to room temperature in 15 min. Samples were studied after 20, 150, 250, and 500 cycles. The life time and the resulting phase composition and microstructural changes were investigated.

(3) Microstructural Characterization

Phase compositions, including the comparative amount of amorphous phase were calculated using the X-ray diffraction (XRD) patterns (D8-Discovery; Bruker AXS, Inc., Madison, WI) and based on the previously mentioned method.[19] This method uses the ratio of the amorphous hump areas to the total peak areas in the entire range of 2θ angles (20–90°), as a scale of the amorphous phase, called amorphous index. Microstructural studies of the coatings and compositional verification of the oxide layers at the interfaces of the coatings were done using field-emission scanning electron microscope (FE-SEM) (Hitachi S4700, Tokyo, Japan) in back-scattered mode. In addition, the average precipitate sizes (formed after heat treatment) were estimated according to 10 measurements at high magnification (100 kX) using the same microscope.

III. Results and Discussion

(1) As-sprayed Coating Microstructure

Figure 1 shows the as coated microstructures of the composite coating. Figure 1(a) exhibits the coating of the composite NAZ (nano-powder mixture) presenting a porous microstructure and loose intersplat bounds. This coating also presented 36% amorphous index, based on the XRD patterns, and calculations (not shown). Figure 1(b) is the coating from spraying the MAZ (micrometer-powder mixture) showing a dense microstructure with well-bounded splats. This coating is of about 64% amorphous index.

(2) Thermal Cycle Testing

Figure 2 exhibits the three coatings on Inconel 625 bond coated with NiCrCoAlY after thermal cyclic testing, including two alumina-YSZ coatings with dense and porous microstructures and the 8 wt% YSZ coating. It was observed that during thermal cyclic test, the high-porosity composite coating exhibiting loose intersplat bond [Fig. 1(a)] failed, i.e., detached entirely from the substrate in less than 20 cycles. By contrast, the dense coating of the same composition [Fig. 1(b)] and the 8 wt% YSZ were still macroscopically attached to the substrate after 500 cycles. This observation suggests that the dense coating of the composite material of alumina-YSZ has the potential for comparatively high performance in cyclic heating.

(3) Coating Failure upon Thermal Cycling

As observed by Chen *et al.*,[3,20] the failure of TBCs in thermal cycling is caused by the crack propagation in the YSZ coating next to and along the YSZ/bond coat interface. The failure occurs through the opening and growth of discontinuities, which is assisted by the crack nucleation and propagation related to the stresses generated by the TGO. It has also been observed that the TGO growth exhibits three distinct

Table II. Spray Conditions for Different Powder Suspensions

Powder	Plasma gas mixture	Total gas (slm), plasma gases ratios, current (A)	Robot speed (m/s)	Plasma power (kW)	$T_p \pm 50$ (°C)	$V_p \pm 20$ (m/s)	Thickness per pass (μm/pass)	Number of passes	Top coat thickness (μm)
MAZ	$Ar/N_2/H_2$	275, 65/15/20, 240	1	103	3050	745	9.0	60	540
NAZ	$Ar/N_2/He$	245, 75/10/15, 200	2	57	3080	612	7.7	60	460
NZ	$Ar/N_2/H_2$	245, 75/10/15, 200	2	86	2950	640	3.4	90	306

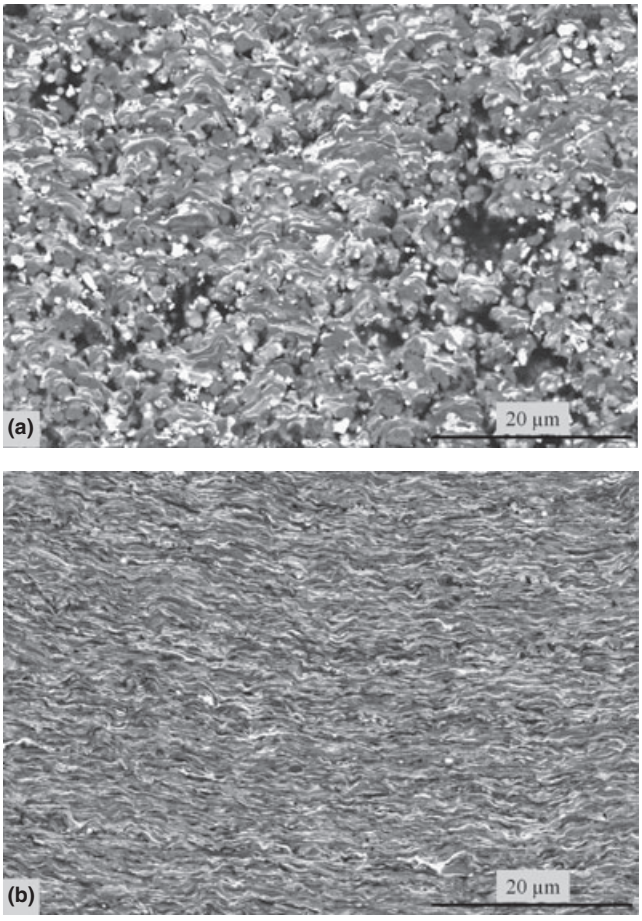

Fig. 1. The microstructure of 60/40 wt% alumina/zirconia SPS coatings generated by (a) NAZ powder and spray condition 2; (b) MAZ powder and spray condition 1.

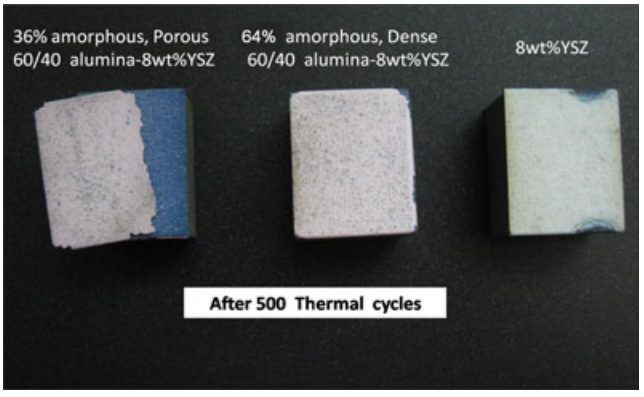

Fig. 2. Thermal cyclic test samples after 500 cycles at 1080°C; left sample with 36% amorphous content (NAZ coating), middle sample with 64% amorphous (MAZ coating), and right sample conventional YSZ (NZ) coating.

stages: (1) an initial TGO growth stage at the onset of oxidation, (2) an intermediary steady-state growth, and (3) a final accelerated growth stage.[20]

It is important to point out that the thermal cycling conditions chosen in this study were close to those employed by Chen *et al.*,[3,20] therefore, it is assumed that the experimental results of this study can be compared to those previously reported. The initial stage of TGO formation for an as-sprayed APS YSZ/CoNiCrAlY TBC occurred at ~20–30 cycles, and this coating failed at ~500 cycles, which corresponded to the third growth stage (i.e., accelerated TGO growth).[20]

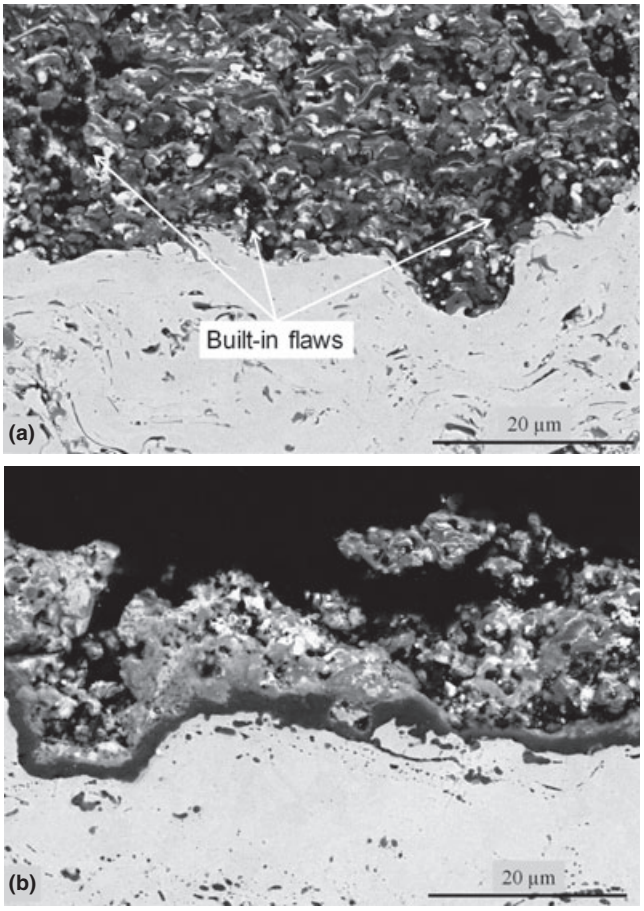

Fig. 3. The interface of the porous composite (NAZ) coating with the bond coat in (a) as-sprayed condition (b) coating failure after 20 thermal cycles.

The porous alumina-YSZ coating failed rapidly in less than 20 cycles, i.e., at the initial stage of TGO growth. The failure occurred within the ceramic coating next to and along the top coat/bond coat interface, i.e., in a similar way as that of a regular TBC. However, the failure occurred during the initial TGO growth and not at the third final accelerated TGO formation stage.

It is likely that the loose intersplat bonding, as observed in Fig. 1(a), allows rapid crack growth by dividing the neighboring splats upon exposure to thermal stresses, in addition to the stresses generated by the TGO and bound coat expansion mismatch. Figure 3(a) shows the as-sprayed interface of this coating with the bond coat including large pores that could act as the built-in flaws, i.e., discontinuities. Figure 3(b) illustrates the coating after failure upon thermal cyclic test. It is possible to observe the growth of a TGO exhibiting the thickness of ~2 μm. It can be seen that the failure has happened within the top coat, next to the top coat/bond coat interface. Due to low intersplat cohesive strength, thermal cycles have resulted in crack propagation, facilitated by bridging between consecutive large pores in the direction parallel to the substrate. Therefore, delamination of the coating occurs before the coating can relax by producing vertical cracks as a means of stress relief.[21]

In contrast, the dense alumina-YSZ and YSZ coatings did not detach from the substrate up to 500 cycles (Fig. 2). It was hypothesized that the dense alumina-YSZ coating would tend to fail after a few thermal cycles due to the stresses induced at high temperatures generated by the crystallization of the amorphous phase in the ceramic. It should be stressed that the thermal cycles have been carried out at temperatures above the crystallization temperature of the amorphous phase in this composite, which is ~950°C.[18] However, the

stronger intersplat cohesion, as previously explained by McPherson,[22] has supported the structure and prevented the visible delaminating of the coatings in the case of dense composite structure, irrespective of the large amorphous content in this coating.

(4) TGO and Spinel Formation

Figure 4 exhibits the as-sprayed and thermally cycled interfaces of the 8 wt% YSZ and alumina-YSZ dense coatings with the bond coats. Figs. 4(a) and (b) are related to the as-sprayed state, which show that, unlike the experience by Chen *et al*. with APS coatings,[23] no noticeable oxide formation or flakes (i.e., discontinuities) exist at the interfaces of SPS coatings. The runs of thermal cyclic heating have resulted in formation of two types of oxides, which are introduced in Fig. 4(c) at the YSZ-bond coat interface. The oxides include an inner dense layer exhibiting dark gray color and an outer micro-porous layer (sometimes clustered) exhibiting light gray color. The EDX evaluation of the oxide layers supported that of previously observed in APS coatings of YSZ.[23] That means the dark oxide layer consists of pure aluminum oxide and the light gray oxide is a mixture of various oxides (spinels) of Al 27.4, Cr 8.6, Co 13.5, and Ni 9.2 atomic percent. Contrary to the continuous aluminum oxide, the mixed oxide presents a very nonuniform and somewhat discontinuous distribution, which makes it difficult to report the thickness. Therefore, for comparison purpose, the maximum thicknesses observed along the length of oxide layer under the microscope were measured here. Based on the literature,[24] the mixed oxide in the TGO plays a major role in crack formation in the TBC.

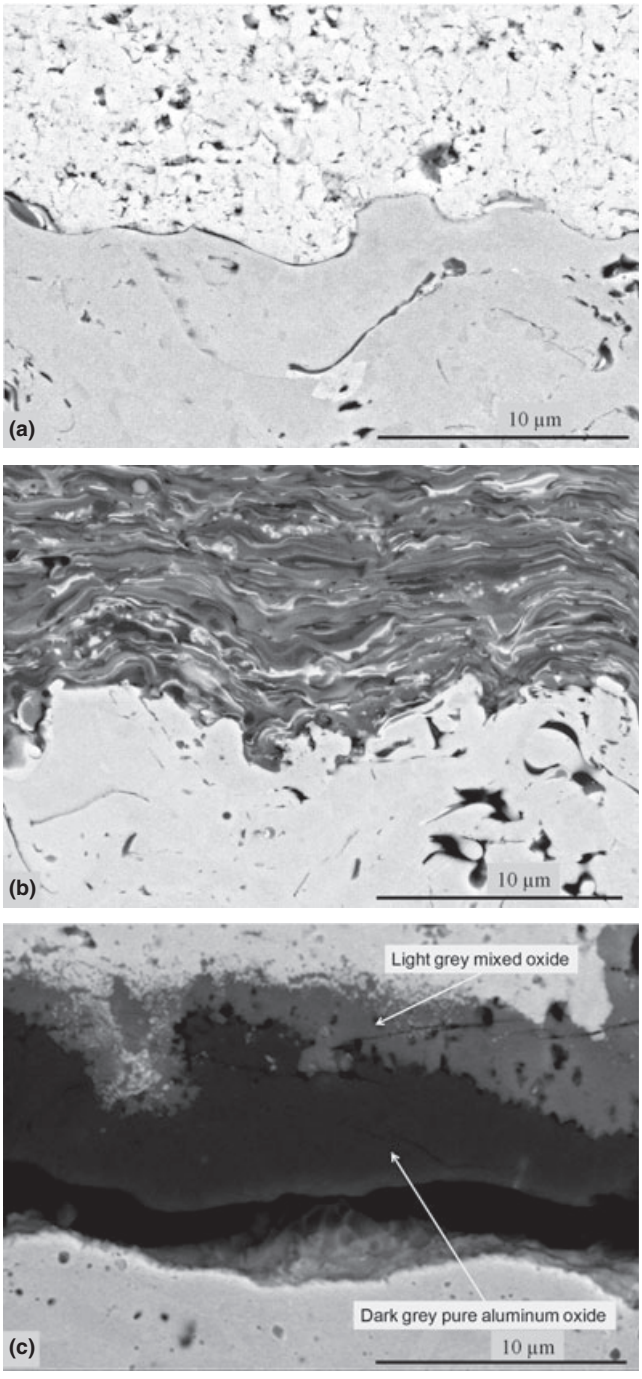

Fig. 4. Top coat/CoNiCrAlY bond coat interface in: (a) as-sprayed 8 wt%YSZ (NZ), (b) as-sprayed alumina-YSZ composite (MAZ), (c) the oxide layers formed in the 8 wt% YSZ during thermal cyclic test.

(5) TGO and Spinel Growth

The TGO growth, for both types of oxides during thermal cyclic test, is summarized in Fig. 5. Figure 5(a) traces the growth of the pure aluminum oxide layer in YSZ and dense alumina-YSZ (MAZ) composite. By looking at Fig. 5(c), it is observed that both coatings exhibited a rapid overall oxide growth (alumina + spinels) immediately after ~20 cycles [Fig. 5 (c)]. Between 20 and 500 cycles, is observed a steady-state growth of the TGO layer, i.e., the initial and intermediary TGO growth stages, as reported by Chen *et al*.[20] As both coatings did not detach after 500 cycles, the third and final accelerated growth of the TGO was not observed.

The overall TGO growth rate of the MAZ composite coating was lower than that of the YSZ [Fig. 5(c)]. One of the reasons for this event was probably the coating porosity. It is known that once the aluminum oxide layer is formed at the interface of the top-bond coat, oxide thickening is dominated by inward diffusion of oxygen atoms through top coat.[25] Moreover, the alumina layers in the YSZ coating have shown to reduce the oxygen diffusion through the top coat.[12] Therefore, it can be assumed that the alumina splats among the YSZ splats in this composite coating have reduced the oxygen diffusion through the top coat, resulting in reduced alumina growth rate at the interface for the first sets of cycles, as well as, the overall TGO growth, up to 500 cycles.

However, after 500 cycles, the extensive cracking of the composite accelerated the growth of pure alumina; therefore, the oxide thicknesses became similar for the two coatings [Fig. 5(a)]. Although the number of the vertical cracks in the two coatings seemed similar, the ones for the composite coating were wider, as observed in Fig. 6. Such crack formation in the composite was also revealed by the uneven surface of this coating, whereas the YSZ exhibited a smoother surface throughout the whole process of thermal cyclic test.

Figure 5(b) represents the maximum thicknesses of the mixed oxide under the two top coats. The same rapid growth as in pure aluminum oxide happens in mixed oxide under both top coats. It should be noted that this thickness, in the composite, is a negligible amount. However, the behavior after this step is different in the composite than the YSZ coating. That means the YSZ presents a constant rate followed by an acceleration period, as previously reported for the YSZ coatings sprayed with APS process.[3] In contrast, the mixed oxide in the case of the composite coating remains constant in a negligible thickness of less than 1 μm. The main reason for the formation of mixed oxides is the aluminum depletion of the bond coat at the interface with top coat.[3,26] The accumulation of the oxygen atoms in this region results in outward migration of the bond coat elements, such as Ni, Cr, and Co through the aluminum oxide layer and formation of mixed oxides. In the composite coating of alumina-YSZ, a large source of free aluminum atoms is

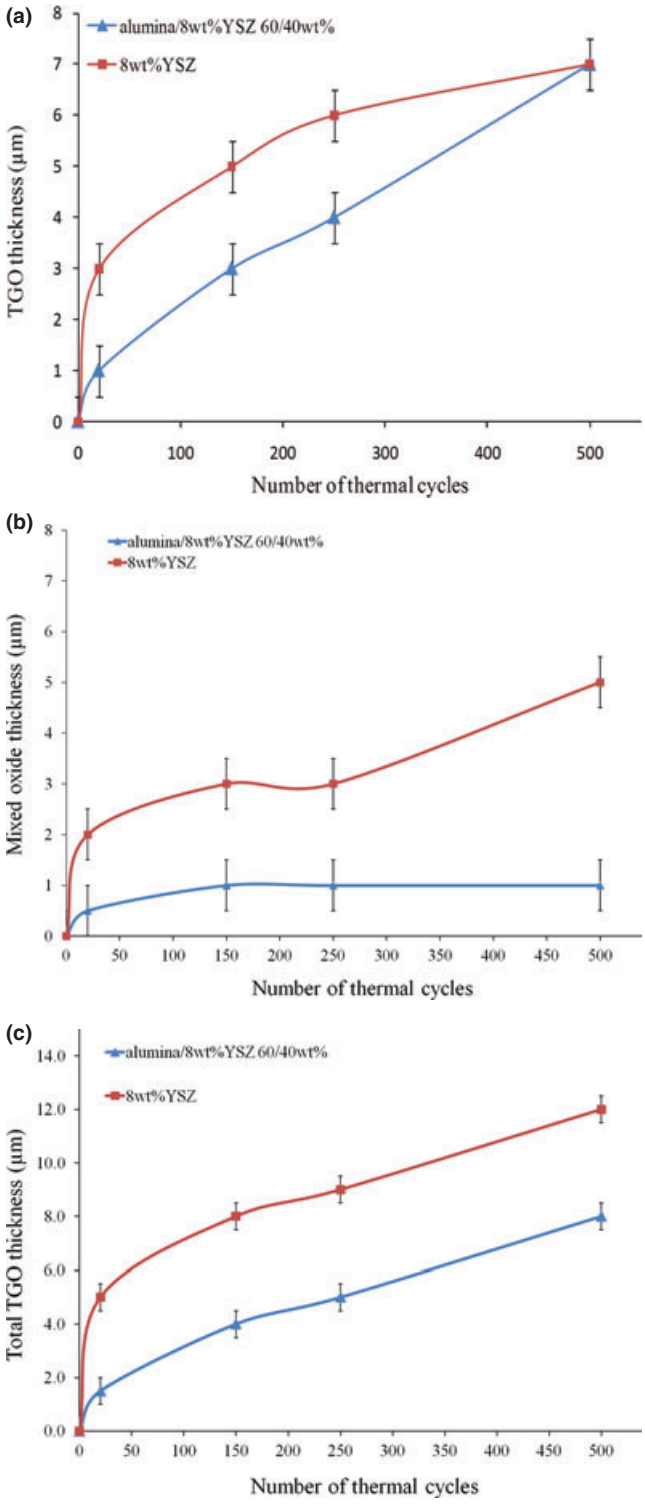

Fig. 5. Growth rates of the TGO oxide layers during thermal cyclic test (a) Aluminum oxide layer (b) Mixed oxide layer (c) Total TGO growth.

provided at the interface during spraying process. They are in the form of dissolved atoms in amorphous phase and or in solid solution with zirconia.[19]

To compare the overall TGO growth in the YSZ coatings deposited by SPS with that of the literature, Fig. 5(c) presents the summation of the two curves of Figs. 5(a) and (b). In general, coatings resulted from SPS process presented lower TGO growth i.e., maximum 12 μm, as compared with an effective thickness of 14 μm that was reported by Chen *et al.*[3] for the YSZ coating deposited by APS process.[3] The effective thickness is the ratio of the total oxide area to the

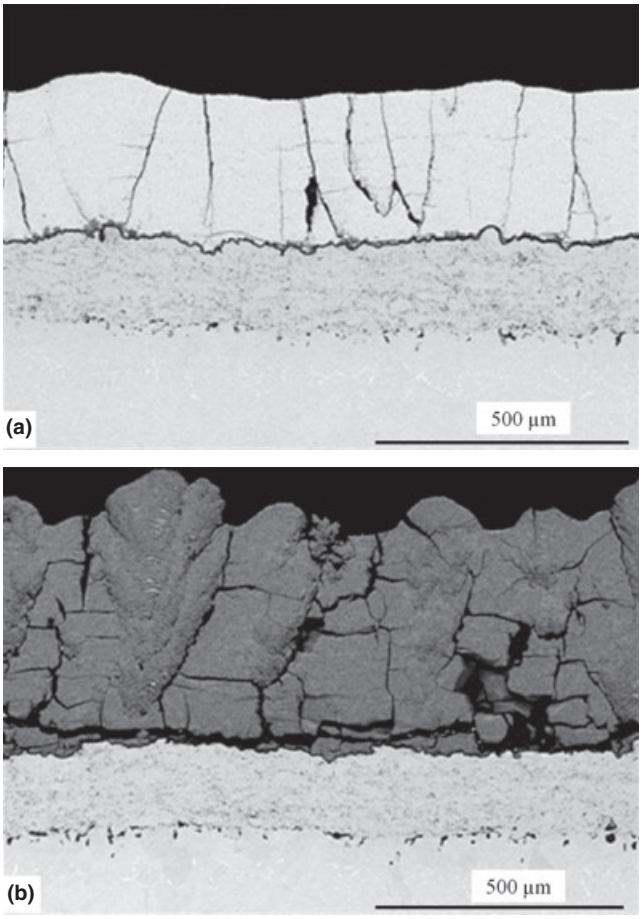

Fig. 6. Samples after 250 thermal cycles (a) with 8 wt% YSZ top coat (b) with alumina-YSZ top coat.

total length of the measurement. In the experiment by Chen *et al.*,[3] the thermal cyclic condition was less severe than that in the present study. That means the APS coatings were tested at heat cycles of 1050°C for 45 min (in this study 1080°C for 1 h cycles). The denser structure with porosities that are of smaller size and more discrete distribution in the SPS coating might be the main reason for less oxygen diffusion and lower TGO growth in these coatings.

Figure 6(b) also infers the extremely brittle nature of the composite with high alumina content by formation of widely opened cracks throughout the structure. This characteristic causes that this coating, in spite of the better resistance to TGO growth, not to be a good choice of TBC. This, however, does not over rule the potential applicability of the composite with lower amounts of alumina phase. It is worth noticing that another reason for severe damage to the composite is the high thermal expansion mismatch with the CoNiCrAlY bond coat which is well designed to match with YSZ.

(6) Phase Transformations

The XRD patterns in Fig. 7 illustrate the structural changes after 500 thermal cycles. Figure 7(a) shows the XRD pattern of the highly amorphous alumina-YSZ composite coating in the as-sprayed condition. It consists of amorphous humps and the crystalline peaks of cubic zirconia and γ-alumina. The present structure is different from that reported by Chen *et al.*,[27] where alumina-zirconia coatings were produced via SPS from amorphous powders. This type of coating exhibited tetragonal zirconia and α-alumina in as-deposited condition.

The long cumulative exposure time at cyclic heat, in the sample after 500 thermal cycles, has resulted in the crystalline

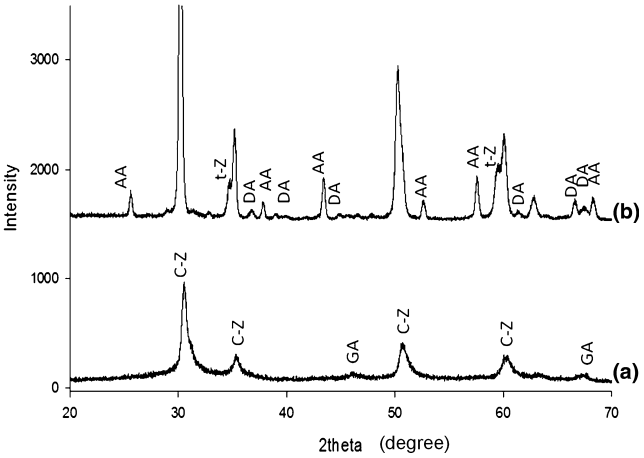

Fig. 7. XRD pattern of high amorphous MAZ sample (64%): (a) as-sprayed and (b) after 500 thermal cycles between room temperature and 1080°C, where C-Z denotes Cubic Zirconia; t-Z, tetragonal zirconia; AA, α-alumina; GA, γ-alumina and DA, δ-alumina.

pattern shown in Fig. 7(b). In this coating, the γ-alumina and the amorphous humps have disappeared and (α + δ)-alumina and (cubic + tetragonal) YSZ are the present phases in the coating after thermal cycling. This is somewhat different from the phases formed during isothermal heat treatment of the coatings at about the same temperatures,[28] where no δ-alumina was observed after 10 h at 1000°C or higher temperatures at 1300°C for 24 h. In fact, the coatings showed no crystallographic changes after 10 h at 1000°C from the initial structure containing α- and/or γ-alumina and cubic zirconia; and after 1300°C for 24 h, the phases included α -alumina and (cubic and/or tetragonal) YSZ.[28] This shows that the phase transformations resulted from heat treatment can be different than thermal cycling at the same approximate temperatures.

In addition, the appearance of α-alumina at such a low temperature is somewhat unexpected. It is in contrast with the results of heat treatment at 1000°C for 12 h,[28] where no alumina transformation could happen and also contrary to the literature that predicts higher transformation temperatures of ~1200°C.[29,30] Thus, formation of α-alumina phases, upon heat treatment, at such a low temperature can most probably be the result of crystallization of amorphous alumina. Comparison of Figs. 7(a) and (b), also, shows the clear peak splitting at 59–60°, which means the tetragonal YSZ structure has become more dominant compared with the cubic phase after this cyclic heating at about crystallization temperature of this high amorphous coating. It should be noticed that both α-alumina and tetragonal YSZ are the stable phases at room temperature; whereas γ-alumina and cubic zirconia are stable at high temperatures and at room temperature they are metastable.

Moreover, it is notable that this composite did not show any formation of monoclinic zirconia, after 500 cycles (i.e., 500 h exposure to 1080°C). This suggests the high resistance to unfavorable phase transformation of zirconia phase in the pseudo-eutectic alumina-YSZ composite coating.

(7) Sintering

Figure 8 allows the comparison of the fracture surfaces of the 8 wt% YSZ (NZ) coating shown in Fig. 8(a) with dense alumina-YSZ composite (MAZ) coatings presented in Fig. 8(b) after 500 thermal cycles. For the YSZ coating [Fig. 8(a)], the splats seemed to have evolved into rounded grains, in a similar way that was observed by Chen *et al.*,[27] for alumina-zirconia coatings heat treated at 1400°C for 2 h. It should be noted that the thinner thickness per deposition

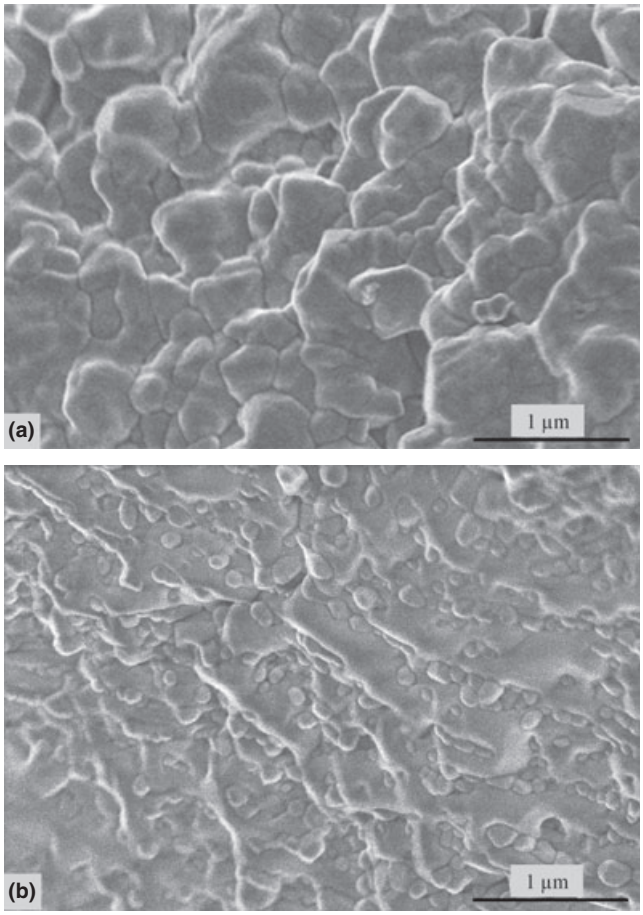

Fig. 8. Fracture surfaces after 500 thermal cycles of: (a) YSZ coating, (b) alumina-YSZ composite coating.

pass of 8 wt% YSZ, observed during this coating process, supports the fact that these splats were not initially larger than the composite (contrary to what can be seen here) in as-sprayed condition.

This observation suggests that the larger YSZ splats compared with the composite, after thermal exposure, are due to its larger proportion of sintering. The larger sintering in YSZ coatings compared with alumina-YSZ composite was previously observed by Dutton *et al.*[31] The reason seems to be that due to limited solubility of the alumina and zirconia,[18] the splats have a low possibility to grow by atomic diffusion through the dissimilar phases. The higher resistance to sintering process can be noted as a great advantage for TBC application, so that the amount of porosity at high temperature, as a controlling parameter on thermal conductivity can be more predictable.

(8) Formation of Nano-Precipitates

The cyclic heating with high heating and cooling rates of the alumina-YSZ composite coating with high amorphous content resulted in an interesting microstructure, not found in isothermal heat treatment of this kind of coating.[28] Figure 9 exhibits the microstructural changes of the high amorphous coating after 500 thermal cycles. The assumingly amorphous portions[18] of the coating structure which are the gray areas of the micrograph in Fig. 9(a) have crystallized into the spotty morphology of Fig. 9(b). As these pictures were taken using the backscattered electron mode, the whitish regions represent Zr-rich regions, whereas, dark regions represent Al-rich regions in the microstructures of the coatings.

It is possible to observe that the thermal cycling induced the precipitation of alumina and zirconia in zirconia and alumina matrixes, respectively [Fig. 9(b)]. The study of the

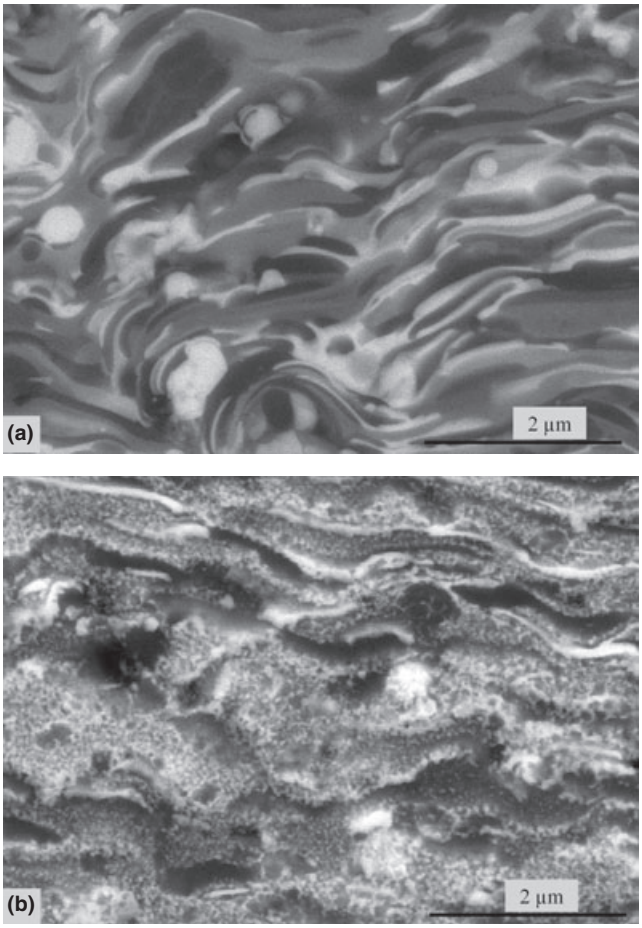

Fig. 9. High amorphous (64% AI) coating of alumina-YSZ composite (a) as-sprayed and (b) after 500 thermal cycles up to 1080°C.

growth rates of the alumina and zirconia precipitates in the high amorphous coating exhibits a parabolic pattern, which is presented in Fig. 10. Due to similar approximate size of the precipitates of each phase into the other (alumina in zirconia matrix and vice versa) a single range of dimensions is reported for both precipitates, related to different number of cycles. During the initial stages of thermal cycles, a rapid growth of precipitates occurs due to the large amount of amorphous phases that have the tendency to crystallize. However, the required thermodynamic condition for crystallization is interrupted due to cyclic process and rapid cooling to room temperatures. Therefore, some retained amorphous phase from the previous steps supports the growth of precipitates up to some specific number of cycles, which in this case is ~200 cycles. At larger number of cycles, when the amorphous phases are no more present in the coating, additional precipitate growth is considerably restricted by the slow diffusion kinetics of the aluminum and zirconium atoms in the crystalline zones of the other phase. This is due to the fact that alumina and zirconia exhibit very limited mutual solid solubility.[32] As a result, the maximum precipitate growth under the conditions employed in this study (500 h at 1080°C which is equal to 500 thermal cycles) is less than 120 nm.

By comparing the present structure of the thermal cyclic test with that of previously observed after isothermal heat treatment,[28] it is possible to observe a basic difference. The alumina precipitates during the isothermal heat treatment at 1200°C for 24 h did not form; whereas, the zirconia precipitates formed and grew to the same approximate size range as in cyclic heat-treated coating after 500 cycles (50 nm). The mechanisms of crystallization and precipitation of the alumina and zirconia have to be responsible for such a difference. Although these mechanisms may be quite complicated, one speculation is as follows. It is expected that during isothermal heat treatment the higher temperature and uninterrupted flow of the migrating atoms during crystallization have allowed the small aluminum atoms to form their alumina crystalline cells adjacent the grains previously formed during deposition. In contrast, the large zirconium atoms could only get a short diffusion path and have formed small precipitates found to be scattered in both heat treatments.

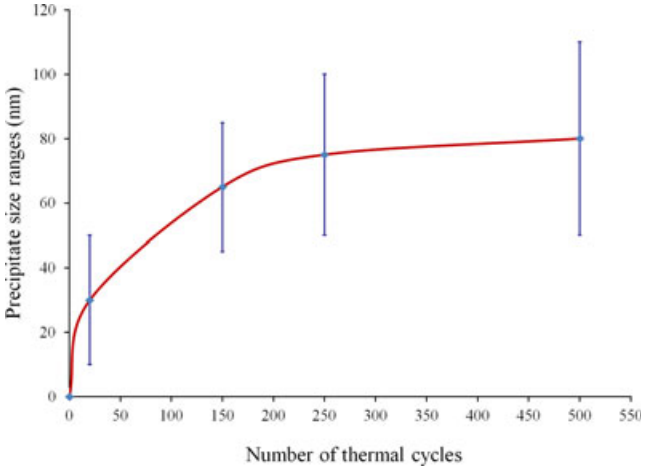

Fig. 10. Growth rate of the nano-precipitates in SPS sprayed alumina-YSZ coating during thermal cyclic testing.

This comparison between the isothermal and cyclic heat treatments of the amorphous-containing composite shows that the precipitates type and size distribution can be engineered using appropriate isothermal treatments and/or thermal cycle lengths and temperatures, from the amorphous phase. The sizes of the precipitates[33] or the second phase[34] in ATZ have shown a considerable role in mechanical properties of the material.

This combined alumina structure with zirconia nano-precipitates, so-called "zirconia toughened alumina" or ZTA, and the alumina nano-precipitates in the zirconia structure known as "alumina hardened zirconia" or AHZ is a "multi-constituent" structure that may benefit the properties of both constituents. The properties of this new structure need to be investigated for various applications. Kirsten *et al.*[15] have previously shown that an extensive amount of alumina dispersed in a zirconia matrix can improve the mechanical long-term reliability in the ATZ (sometimes referred as AHZ) materials as potentials for medical applications. Such structure also may be used in solid oxide fuel cells (SOFC), as Bucko *et al.*[33] studied the alumina-zirconia composite for SOFC in the form of alumina inclusions in cubic zirconia. It was observed that the highest increase in fracture toughness can be found when the inclusion size was comparable to the matrix grain sizes. This condition of comparable particle sizes of alumina and zirconia (as observed in the SEM micrographs in this study [e.g., Fig. 9(b)], exists in the present structure. In addition, the prominent zirconia structure resulted from the SPS coating of the alumina-YSZ is the cubic phase.[35] Moreover, Mondal[36] investigated the ZTA as the favorite cutting tool for machining steels and cast iron, which is of enhanced strength and toughness than plain ceramics.

This multi-constituent structure may be used in some of the above or many other applications, after necessary exploration of the required properties. In addition, based on this experiment, a production route for the composites with nano-precipitate dispersion with hardening or toughening characteristics, along with high stability of the size distribution can be introduced. This may be achieved through the isothermal heat treatment and/or thermal cyclic heat treatments of the

amorphous phases for many other ceramic systems with limited solubility, like in alumina-zirconia system. The amorphous phases were formed here during high cooling rate processes like plasma spray coating. However, this does not override the possibility for the use of amorphous phases formed during other production processes for this purpose.

IV. Conclusions

The SPS coatings were subjected to thermal cycling. The materials of study included the 8 wt% YSZ, which is the state-of-the-art TBC top coat, and the ceramic composite of alumina-8 wt% YSZ with pseudo-eutectic composition. It was found that the composite may survive up to 500 cycles at 1080°C without detachment from the substrate. However, it exhibits a brittle behavior that does not make it a good choice of TBC. Nevertheless, the composite coating shows an enhanced resistance to the TGO growth and especially to the harmful mixed oxide growth. Accordingly, the investigation of the composite with the lower alumina content is recommended. The XRD studies showed that the crystalline structure resulted from isothermal heat treatment can be different from that of thermal cyclic process, especially in the amorphous containing material. In addition, high temperature phase stability for the cubic and or tetragonal zirconia is found in the presence of alumina which adds up with the stabilizing role of yttria. Regarding the sintering phenomena, the alumina phase between the YSZ splats reduces the sintering effect of YSZ.

A new multi-constituent structure was fabricated, which is composed of alumina hardened zirconia (AHZ) and zirconia toughened alumina (ZTA). This coating may benefit the characteristics of both structures (either AHZ or ZTA), while enjoying the privilege of nano-precipitate dispersion. This structure is produced by cyclic heating of the largely amorphous coatings. Heating cycles were in a range between room temperature and 1080°C, which is slightly above crystallization temperature of the composite (~950°C). Accordingly, an effective method for production of nano-crystalline structure in ceramic composite coatings was suggested. The method is based on the amorphous phase and its crystallization in solid state.

Acknowledgment

The authors express their appreciation to the Liburdi Engineering (Dundas, ON, Canada), especially Mr. Doug Nagy and Dr. Tiberius Rusan de Priamus, for supporting this research by performing the thermal cyclic tests in their laboratory.

References

[1]M. Yashima, T. Nagatome, T. Noma, N. Ishizawa, Y. Suzuki, and M. Yoshimura, "Effect of Dopant Species on Tetragonal (t') to Monoclinic Phase Transformation of Arc-Melted ZrO_2-$RO_{1.5}$ (R = Sm, Y, Er, and Sc) in Water at 200° C and 100 MPa Pressure," *J. Am. Ceram. Soc*., **78**, 2229–32 (1995).

[2]M. Yashima, M. Kakihana, and M. Yoshimura, "Metastable-Stable Phase Diagrams in the Zirconia-Containing Systems Utilized in Solid-Oxide Fuel Cell Application," *Solid State Ionics*, **86–88**, 1131–49 (1996).

[3]W. R. Chen, X. Wu, B. R. Marple, and P. C. Patnaik, "The Growth and Influence of Thermally Grown Oxide in a Thermal Barrier Coating," *Surf. Coat. Technol*., **201**, 1074–9 (2006).

[4]J. A. Haynes, M. K. Ferber, and W. D. Porter, "Thermal Cycling Behavior of Plasma-Sprayed Thermal Barrier Coatings With Various MCrAlX Bond Coats," *J. Therm. Spray Technol*., **9**, 38–48 (2000).

[5]T. Troczynski, Q. Yang, and G. John, "Post-Deposition Treatment of Zirconia Thermal Barrier Coatings Using Sol-Gel Alumina," *J. Therm. Spray Technol*., **8**, 229–34 (1999).

[6]A. Afrasiabi, M. Saremi, and A. Kobayashi, "A Comparative Study on Hot Corrosion Resistance of Three Types of Thermal Barrier Coatings: YSZ, YSZ + Al_2O_3 and YSZ/Al_2O_3," *Mater. Sci. Eng., A*, **478**, 264–9 (2008).

[7]M. Saremi, A. Afrasiabi, and A. Kobayashi, "Microstructural Analysis of YSZ and YSZ/Al_2O_3 Plasma Sprayed Thermal Barrier Coatings After High Temperature Oxidation," *Surf. Coat. Technol*., **202**, 3233–8 (2008).

[8]G. Shanmugavelayutham, S. Yano, and A. Kobayashi, "Microstructural Characterization and Properties of ZrO_2/Al_2O_3 Thermal Barrier Coatings by Gas Tunnel-Type Plasma Spraying," *Vacuum*, **80**, 1336–40 (2006).

[9]S. Sharafat, A. Kobayashi, V. Ogden, and N. M. Ghoniem, "Development of Composite Thermal Barrier Coatings With Anisotropic Microstructure," *Vacuum*, **59**, 185–93 (2000).

[10]P. Ramaswamy, S. Seetharamu, K. B. R. Varma, and K. J. Rao, "Al_2O_3-ZrO_2 Composite Coatings for Thermal-Barrier Applications," *Compos. Sci. Technol*., **57**, 81–9 (1997).

[11]S. Widjaja, A. M. Limarga, and T. H. Yip, "Modeling of Residual Stresses in a Plasma-Sprayed Zirconia/Alumina Functionally Graded-Thermal Barrier Coating," *Thin Solid Films*, **434**, 216–27 (2003).

[12]A. M. Limarga, S. Widjaja, and T. H. Yip, "Mechanical Properties and Oxidation Resistance of Plasma-Sprayed Multilayered Al_2O_3/ZrO_2 Thermal Barrier Coatings," *Surf. Coat. Technol*., **197**, 93–102 (2005).

[13]F. Tarasi, M. Medraj, A. Dolatabadi, J. Oberste-Berghaus, and C. Moreau, "Structural Considerations During Atmospheric Plasma Spraying of the Alumina-Zirconia Composite," *Surf. Coat. Technol*., **205**, 23–24, 5437–43 (2011).

[14]F. Tarasi, M. Medraj, A. Dolatabadi, J. Oberste-Berghaus, and C. Moreau, "Phase Formation and Transformations in Alumina-YSZ Nano-Composite Coating Deposited by Suspension Plasma Spray Process," *J. Therm. Spray Technol*., **19** [4] 787–95 (2010).

[15]A. Kirsten, S. Begand, T. Oberbach, R. Telle, and H. Fischer, "Subcritical Crack Growth Behavior of Dispersion Oxide Ceramics," *J. Biomed. Mater. Res. B Appl. Biomater*., **95B**, 202–6 (2010).

[16]J. Schneider, S. Begand, R. Kriegel, C. Kaps, W. Glien, and T. Oberbach, "Low-Temperature Aging Behavior of Alumina-Toughened Zirconia," *J. Am. Ceram. Soc*., **91**, 3613–8 (2008).

[17]L. G. J. Chevalier, "Ceramics for Medical Applications: A Picture for the Next 20 Years," *J. Eur. Ceram. Soc*., **29**, 1245–55 (2009).

[18]F. Tarasi, M. Medraj, A. Dolatabadi, J. Oberste-Berghaus, and C. Moreau, "Amorphous and Crystalline Phase Formation During Suspension Plasma Spraying of Alumina-YSZ Composite Coatings," *J. Eur. Ceram. Soc*., **31** [15] 2903–13 (2011).

[19]F. Tarasi, "*Suspension Plasma Sprayed Alumina-Yttria Stabilized Zirconia Nano-Composite Thermal Barrier Coatings - Formation and Roles of the Amorphous Phase*"; PhD thesis, Concordia University, Montreal, Canada, 2010.

[20]W. R. Chen, X. Wu, B. R. Marple, R. S. Lima, and P. C. Patnaik, "Pre-Oxidation and TGO Growth Behaviour of an Air-Plasma-Sprayed Thermal Barrier Coatings," *Surf. Coat. Technol*., **202**, 3787–96 (2008).

[21]Q. Zhang, C.-J. Li, Y. Li, S.-L. Zhang, X. R. Wang, G.-J. Yang, and C.-X. Li, "Thermal Failure of Nanostructured Thermal Barrier Coatings With Cold-Sprayed Nanostructured NiCrAlY Bond Coat," *J. Therm. Spray Technol*., **17**, 838–45 (2008).

[22]R. S. Lima and B. R. Marple, "Toward Highly Sintering-Resistant Nanostructured ZrO_2-7wt.%Y_2O_3 Coatings for TBC Applications by Employing Differential Sintering," *J. Therm. Spray Technol*., **17**, 846–52 (2008).

[23]W. R. Chen, X. Wu, D. Dudzinski, and P. C. Patnaik, "Modification of Oxide Layer in Plasma-Sprayed Thermal Barrier Coatings," *Surf. Coat. Technol*., **200**, 5863–8 (2006).

[24]Y. Li, C.-J. Li, Q. Zhang, G.-J. Yang, and C.-X. Li, "Influence of TGO Composition on the Thermal Shock Lifetime of Thermal Barrier Coatings With Cold-Sprayed MCrAlY Bond Coat," *J. Therm. Spray Technol*., **19**, 168–77 (2010).

[25]A. G. Evans, D. R. Clarke, and C. G. Levi, "The Influence of Oxides on the Performance of Advanced Gas Turbines," *J. Eur. Ceram. Soc*., **28**, 1405–19 (2008).

[26]M. H. Li, Z. Y. Zhang, X. F. Sun, H. R. Guan, W. Y. Hu, and Z. Q. Hu, "Oxidation and Degradation of EB-PVD Thermal-Barrier Coatings," *Oxid. Met*., **58**, 499–512 (2002).

[27]D. Chen, E. H. Jordan, and M. Gell, "Suspension Plasma Sprayed Composite Coating Using Amorphous Powder Feedstock," *Appl. Surf. Sci*., **255**, 5935–8 (2009).

[28]F. Tarasi, M. Medraj, A. Dolatabadi, J. Oberste-Berghaus, and C. Moreau, "High-Temperature Performance of Alumina-Zirconia Composite Coatings Containing Amorphous Phases," *Adv. Funct. Mater*., **21** [21] 4143–51 (2011).

[29]R. J. Damani and P. Makroczy, "Heat Treatment Induced Phase and Microstructural Development in Bulk Plasma Sprayed Alumina," *J. Eur. Ceram. Soc*., **20**, 867–88 (2000).

[30]R. McPherson, "On the Formation of Thermally Sprayed Alumina Coatings," *J. Mater. Sci*., **15**, 3141–9 (1980).

[31]R. Dutton, R. Wheeler, K. S. Ravichandran, and K. An, "Effect of Heat Treatment on Thermal Conductivity of Plasma-Sprayed Thermal Barrier Coatings," *J. Therm. Spray Technol*., **9**, 204–9 (2000).

[32]V. Jayarama, C. G. Levia, T. Whitneya, and R. Mehrabiana, "Characterization of Al_2O_3-ZrO_2 Powders Produced by Electrohydrodynamic Atomization," *Mater. Sci. Eng., A*, **124**, 65–81 (1990).

[33]M. M. Bucko and W. Pyda, "Effect of Inclusion Size on Mechanical Properties of Alumina Toughened Cubic Zirconia," *J. Mater. Sci*., **40**, 5191–8 (2005).

[34]D. Casellas, M. M. Nagl, L. Llanes, and M. Anglada, "Microstructural Coarsening of Zirconia-Toughened Alumina Composites," *J. Am. Ceram. Soc*., **88**, 1958–63 (2005).

[35]F. Tarasi, M. Medraj, A. Dolatabadi, J. Oberste-Berghaus, and C. Moreau, "Phase Formation and Transformation in Alumina/YSZ Nanocomposite Coating Deposited by Suspension Plasma Spray Process," *J. Therm. Spray Technol*., **9**, 787–95 (2010).

[36]B. Mondal, "Zirconia Toughened Alumina for Wear Resistant Engineering and Machinability of Steel Application," *Adv. Appl. Cerm.: Struct. Funct. Bioceram*, **104**, 256–60 (2005). □